

Electronic Supplementary Information

Mirror Symmetry Origin of Dirac Cone Formation in Rectangular Two-dimensional Materials

*Xuming Qin^{*a}, Yi Liu^{*b}, Gui Yang^a, and Dongqiu Zhao^a*

^aSchool of Physics and Electrical Engineering, Anyang Normal University, Anyang
455000, P. R. China

^bMaterials Genome Institute, Shanghai University, 333 Nanchen Road, Shanghai
200444, P. R. China

E-mail: xmqin@aynu.edu.cn (Xuming Qin);

E-mail: yiliu@shu.edu.cn (Yi Liu)

S1 Origin of the Dirac Cone along the path MX of 6,6,12-graphyne

Similar to the analysis of the origin of the Dirac cone (DC) along the path $k_y = 0$ ($\Gamma X'$) in the manuscript, the origin of the DC along the path $k_y = \pm\pi/b$ (MX) can also be analyzed by a similar “mirror symmetry parity coupling (MSPC)” method.

Firstly, the “original Bloch vectors” (OBV) obtained in the manuscript can be divided into four parts: $G1^{++}$, $G2^{++}$, $G1^{-}$, and $G2^{-}$ according to which atoms are derived and their parity along the path $k_y = \pm\pi/b$. $G1^{++}$ (originating from G1 and having even parity relative to the line $y=b/2$ when $k_y = \pm\pi/b$) include:

$$|rp^{-+}\rangle_k, |rp^{--}\rangle_k, |rs^{-+}\rangle_k, |b^{++}\rangle_k \quad (S1)$$

$G2^{++}$ (originating from G2 and having even parity relative to the line $y=b/2$ when $k_y = \pm\pi/b$) include:

$$|chp^{++}\rangle_k, |chp^{+-}\rangle_k, |chr^{++}\rangle_k, |chr^{+-}\rangle_k, |p^{++}\rangle_k \quad (S2)$$

$G1^{-}$ (Originating from G1 and having odd parity relative to the line $y=b/2$ when $k_y = \pm\pi/b$) include:

$$|rp^{++}\rangle_k, |rp^{+-}\rangle_k, |rs^{++}\rangle_k, |b^{-+}\rangle_k \quad (S3)$$

$G2^{-}$ (Originating from G2 and having odd parity relative to the line $y=b/2$ when $k_y = \pm\pi/b$) include:

$$|chp^{-+}\rangle_k, |chp^{--}\rangle_k, |chr^{-+}\rangle_k, |chr^{--}\rangle_k, |p^{-+}\rangle_k \quad (S4)$$

For ease of expression, the combination of $G1^{++}$ and $G2^{++}$ is marked G^{++} , the combination of $G1^{-}$ and $G2^{-}$ is marked G^{-} .

In the Brillouin zone, when $k_y = \pm\pi/b$, there are no intragroup couplings between G^{++} and G^{-} due to the different parities.

As described in the manuscript, the formation processes of the DC along the path $\Gamma X'$ of 6,6,12-graphyne can be schematically described in Fig. 4; similarly, the formation process of the DC along the path MX can be shown in Fig. S1, where, $G1^{++}_0$ et al. are defined similarly as in the manuscript and are shown in Fig. S2. $G2^{++}$ and $G2^{-}$ are the same as $G2^{+}$ and $G2^{-}$, respectively; so, $G2^{++}_0$ bands, $G2^{++}_1$ bands, $G2^{-}_0$ bands, and $G2^{-}_1$ bands are same as $G2^{+}_0$ bands, $G2^{+}_1$ bands, $G2^{-}_0$ bands, and $G2^{-}_1$ bands, respectively. In $G1^{++}$, $|rp^{-+}\rangle_k$ and $|rp^{--}\rangle_k$ are anti-bonding states, $|b^{++}\rangle_k$ is bonding state, and $|rs^{-+}\rangle_k$ is neither bonding state nor anti-bonding states; so, there are one band lower than the Fermi-level, two bands higher than the Fermi-level, and one band near the Fermi-level in $G1^{++}_0$, and there are two bands higher than the Fermi-level and two bands lower than the Fermi-level in $G1^{++}_1$. While, there are three bands lower than the Fermi-level, two bands higher than the Fermi-level in $G2^{++}_1$; so, the intergroup couplings between $G1^{++}_1$ bands and $G2^{++}_1$ bands make valence band (VB) bend upward (In $G1^{++}_1$ and $G2^{++}_1$ bands, the total number of bands lower than the Fermi-level is more than the total number of bands higher than the Fermi-level).

Similarly, there are two bands lower than the Fermi-level, one band higher than the Fermi-level, and one band near the Fermi-level in $G1^{-'0}$, and there are two bands higher than the Fermi-level and two bands lower than the Fermi-level in $G1^{-'1}$. While, there are three bands higher than the Fermi-level and two bands lower than the Fermi-level in $G2^{-'1}$; so, the intergroup couplings between $G1^{-'1}$ bands and $G2^{-'1}$ bands make conduction band (CB) bends downward and intersect with VB. The intersection lines in the k space are a group of periodic tiny ellipse-like closed curves, of which there are two half-closed curves intersecting with the path MX at A point in the Brillouin zone, shown in Fig. S2 (k). At last, the intergroup couplings between $G^{+'2}$ bands and $G^{-'2}$ bands lead to the formation of the DC in the path MX. The various band structures in the formation processes of the DC along the path MX are shown in Fig. S2.

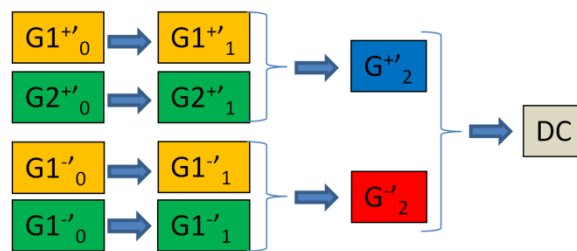


Fig. S1 The schematic formation process of the DC along the path MX of 6,6,12-graphyne.

The bridge atoms labeled 7 and 8 play an important role in the formation of the DC in the path XM. If the C atoms in the bridge are substituted by H atoms (the new system is named as 6 (H2), 14,18 graphyne¹), the number of the bands below the Fermi-level in $G1^{+'1}$ will change into one from two, and the upward bending of VB caused by the intergroup couplings between $G1^{+'1}$ bands and $G2^{+'1}$ bands becomes very weak; similar, the number of the band above the Fermi-level in $G1^{-'1}$ will change into one from two, and the downward bending of CB caused by the intergroup couplings between $G1^{-'1}$ bands and $G2^{-'1}$ bands also becomes very weak. Then CB and VB can not intersect and the DC in the path XM can not be formed. The corresponding formation process of the band structure is shown in Fig. S3 (The same TB parameters and Brillouin zone as 6,6,12-graphyne are adopted)

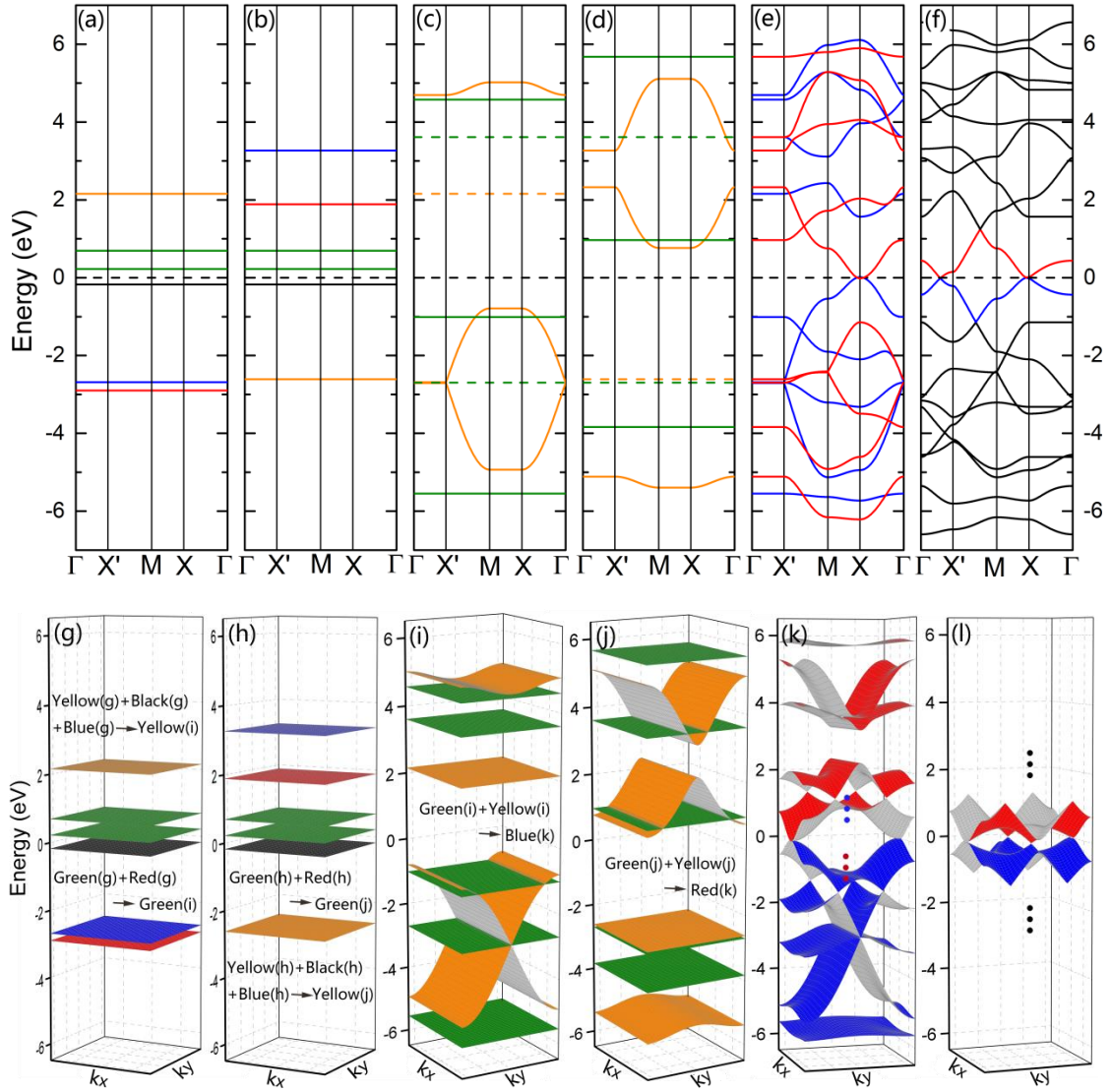


Fig. S2 The formation procession of the DC along the path MX of 6,6,12-graphyne. (a, g) $G1^{+0}$ bands in black, yellow and blue lines and $G2^{+0}$ bands in green and red lines. (b, h) $G1^{-0}$ band in black, yellow and blue lines and $G2^{-0}$ bands in green and red lines. (c, i) $G1^{+1}$ bands in yellow lines and $G2^{+1}$ bands in green lines. (d, j) $G1^{-1}$ bands in yellow lines and $G2^{-1}$ bands in green lines. (e, k) G^{+2} bands in blue lines and G^{-2} bands in red lines. (f, l) The band structure of 6,6,12-graphyne with DC along the path MX is formed with the intergroup couplings between the G^{+} and G^{-} considered.

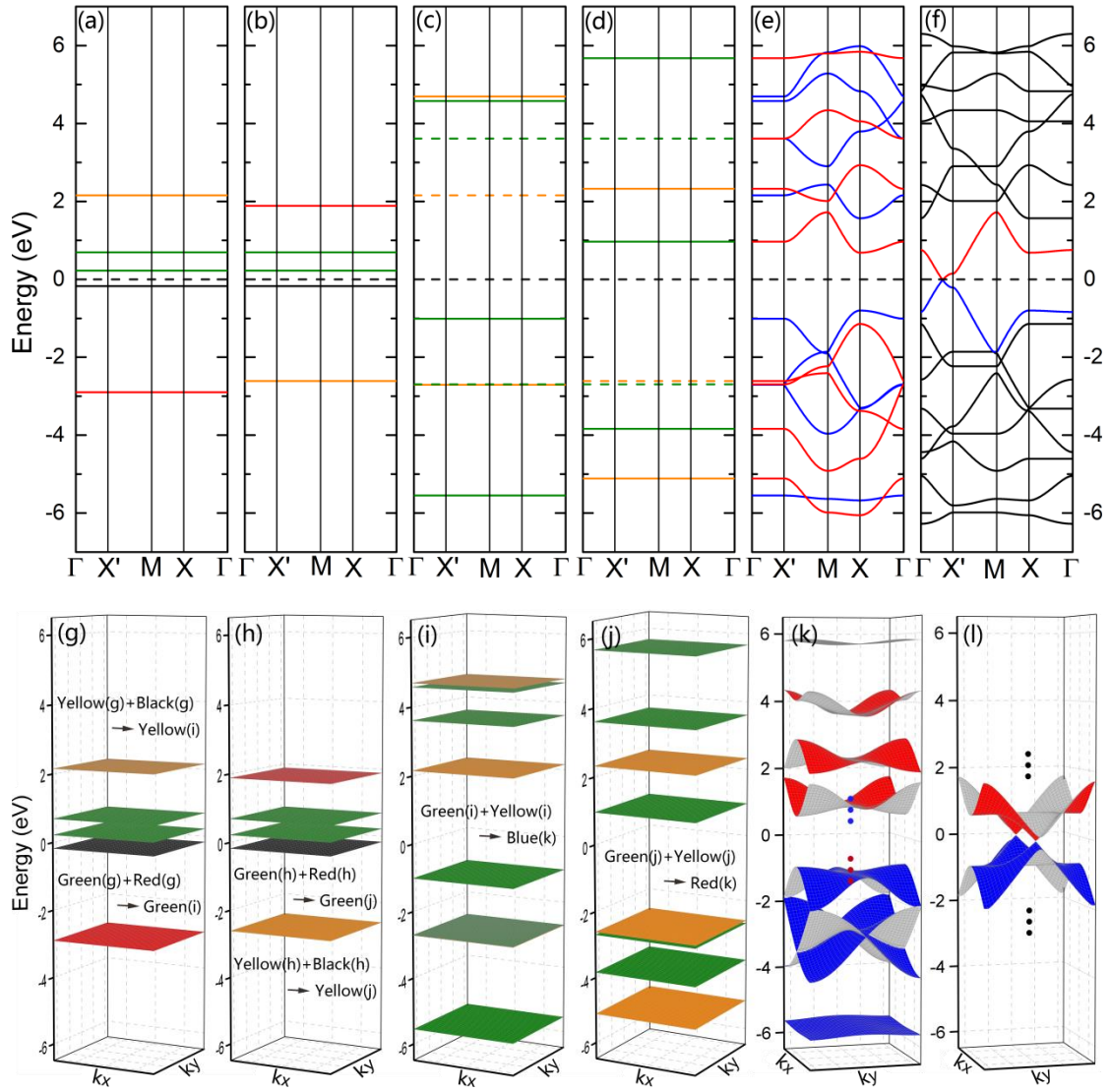


Fig. S3 The schematic illustration for explaining why there are no DCs along the Path MX for 6 (H2), 14,18 graphyne. (a, g) $G1^{+0}$ bands in black, yellow and blue lines and $G2^{+0}$ bands in green and red lines. (b, h) $G1^{-0}$ band in black, yellow and blue lines and $G2^{-0}$ bands in green and red lines. (c, i) $G1^{+1}$ bands in yellow lines and $G2^{+1}$ bands in green lines. (d, j) $G1^{-1}$ in yellow lines and $G2^{-1}$ bands in green lines. (e, k) G^{+2} bands in blue lines and G^{-2} bands in red lines. (f, l) The band structure of 6 (H2), 14,18 graphyne with no DC along the path MX is formed with the intergroup couplings between G^{+} and G^{-} considered.

S2 Atom structures of the derivatives of 6,6,12-graphyne by DFT

Based on 6,6,12-graphyne, a series of derivatives of 6,6,12-graphyne can be obtained by substituting or adding some atoms. Their atom structures after geometric optimization by DFT calculations are shown in Fig. S4, Fig. S5, Fig. S6, and Fig. S7. The bridging atoms (labeled with 7 and 8 in the manuscript) in 6,6,12-graphyne are replaced by hydrogen atoms to obtain the system 6 (H2), 14,18 graphyne shown in

Fig. S4 (a). In addition, on the basis of 6 (H2), 14, 18 graphyne, a new system 6 (H2), 14, 18 graphyne-ch-N (abbreviated as ch-N with 6 (H2), 14, 18 graphyne being abbreviated as ch-2 in this work) shown in Fig. S4 can be acquired when N-2 carbon atoms are inserted simultaneously between the chain atoms (between the atoms labeled with 11 and 12, 13 and 14, 15 and 16 as well as 17 and 18 in the manuscript). While on the basis of ch-2, a new system 6 (H2), 14, 18 graphyne-p-N (abbreviated as p-N in this work) shown in Fig. S5 with N-2 atoms inserted between the pair atoms (labeled 9 and 10 in the manuscript) can be acquired. sch-2 shown in Fig. S6 (a) can be obtained by replacing the hexagon ring of ch-2 with carbon atom pairs. Similar to ch-N, on the basis of sch-2, sch-N shown in Fig. S6 can be acquired when N-2 carbon atoms are inserted simultaneously between the chain atoms. While similar to p-N, on the basis of sch-2, sp-N shown in Fig. S7 can be acquired when N-2 carbon atoms are inserted between the pair atoms. In the DFT calculations, the same computation parameters were adopted as those of 6,6,12-graphyne in the manuscript except for the Monkhorst-Pack k point samplings for the systems sch-2 ($7\times 7\times 1$), sch-3 ($7\times 7\times 1$), sp-3 ($7\times 7\times 1$), sp-4 ($7\times 5\times 1$), and sp-5 ($7\times 5\times 1$) in the SCF calculations.

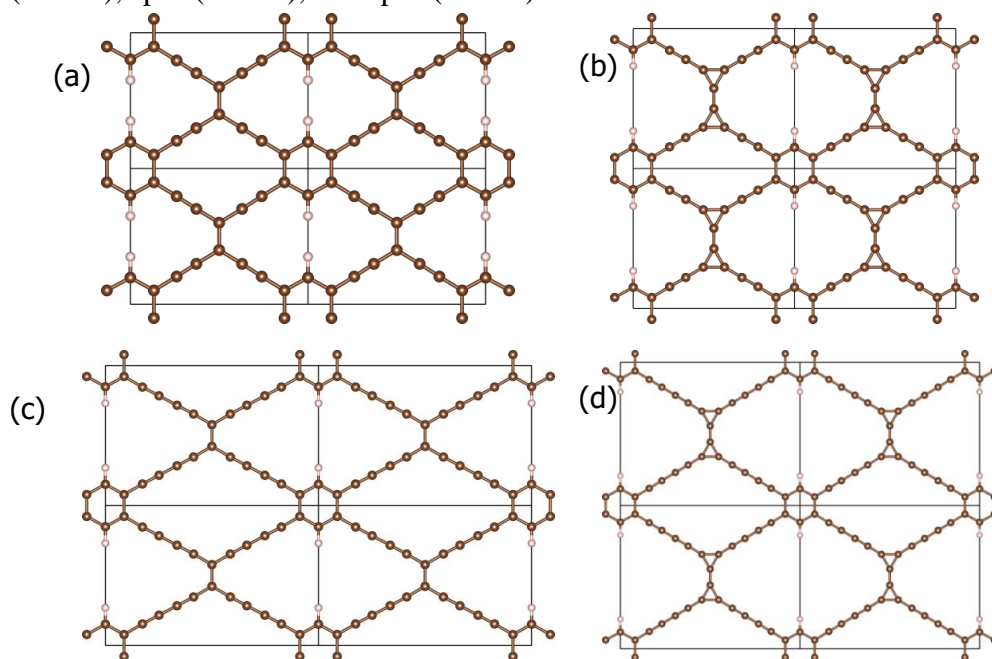


Fig. S4 Atomic structures of ch-N. (a) ch-2. (b) ch-3. (c) ch-4. (d) ch-5.

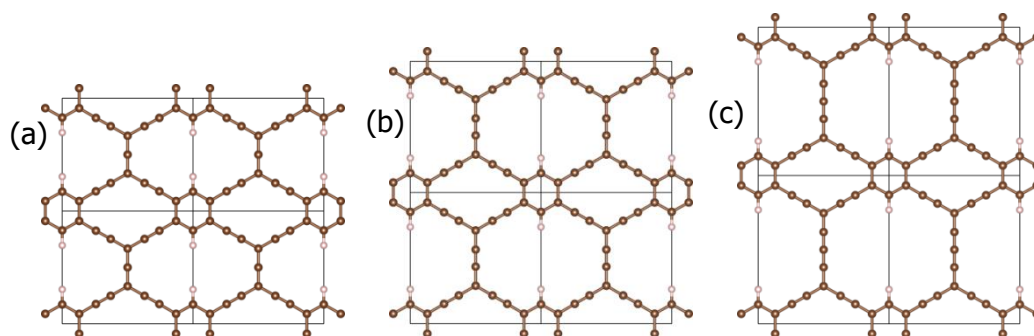


Fig. S5 Atomic structures of p-N. (a) p-3. (b) p-4. (c) p-5.

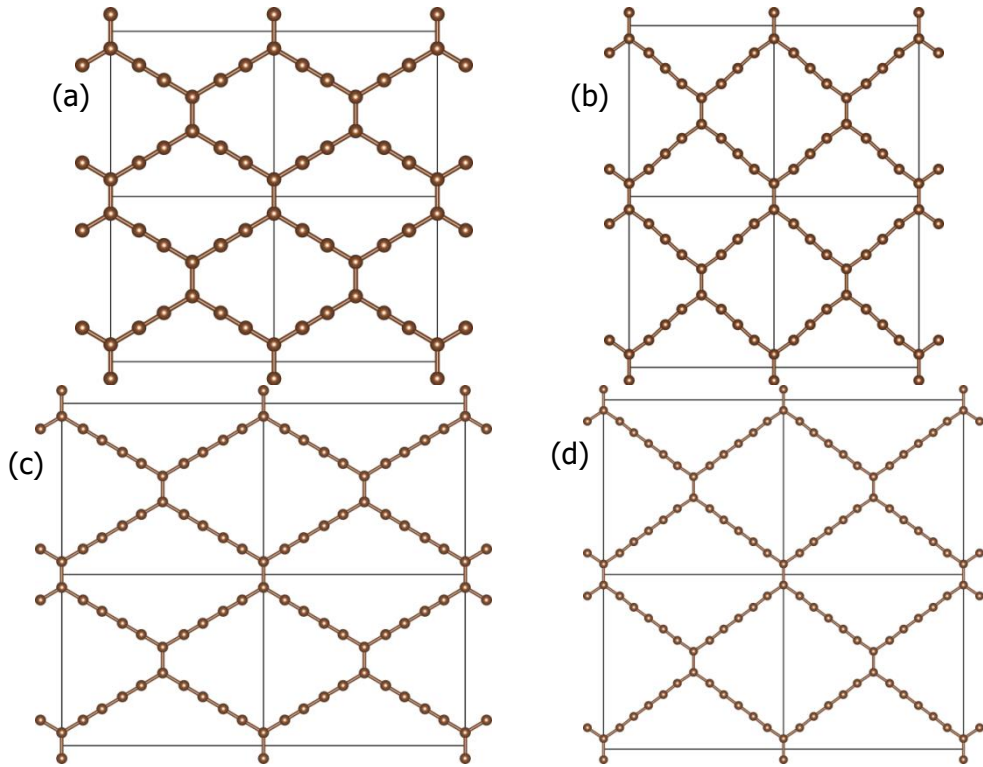


Fig. S6 Atomic structures of sch-N. (a) sch-2. (b) sch-3. (c) sch-4. (d) sch-5.

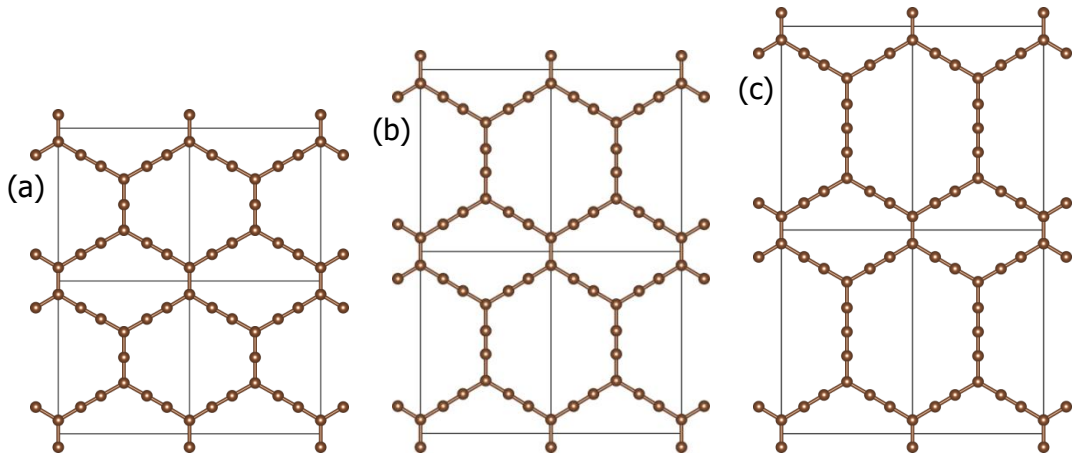


Fig. S7 Atomic structures of sp-N. (a) sp-3. (b) sp-4. (c) sp-5.

S3 Predictions on whether the derivatives of 6,6,12-graphyne possesses DC band structures and the band structures of the derivatives of 6,6,12-graphyne by DFT

Based on the analysis of the formation process of the DC band structure of 6,6,12-graphyne, it can be predicted whether some derivatives of 6,6,12-graphyne possess DCs.

S3.1 ch-N

For ch-N, they should not have DC along the path $k_y = \pm\pi/b$. the reason is that: Similar with 6,6,12-graphyne, the bands higher than the Fermi-level are more than the bands lower than the Fermi-level in $G1^{+\prime}_1$, and the bands lower than the Fermi-level are more than the bands higher than the Fermi-level in $G2^{+\prime}_1$, so the upward bending of VB caused by the intergroup couplings between $G1^{+\prime}_1$ bands and $G2^{+\prime}_1$ bands is very weak; the bonding states in $G1^{-\prime}_1$ are more than anti-bonding states, and the anti-bonding states in $G2^{-\prime}_1$ are more than bonding states, so the downward bending of CB caused by the couplings between $G1^{-\prime}_1$ bands and $G2^{-\prime}_1$ bands is very weak. Then CB and VB cannot intersect, and the DC in the path $k_y = \pm\pi/b$ cannot be formed.

Refer to along the path $k_y = 0$, when N is even, ch-N possess DC, while when N is odd, ch-N does not possess DC. This can be explained as: when N is even, for example, N is four, $G2^{+0}$ includes nine bands, of which, one band is from pair atoms, eight bands are from chain atoms which are near the Fermi-level. The eight bands can be divided into two segments, segment 1 possesses even parity relative to $x = a/2 + ha$ in each cell, and segment 2 possesses odd parity relative to $x = a/2 + ha$ in each cell. The intragroup couplings of segment 2 (or segment 1) produce four new bands, of which, two bands are under the Fermi-level, and two bands are above the Fermi-level. The intergroup couplings between the four new bands from segment 1 and the band from the pair atoms which possess even parity relative to $x = a/2 + ha$ in each cell produce five new bands, of which, three bands are under the Fermi-level, two bands are above the Fermi-level. At last, $G2^{+1}$ includes nine bands, of which, five bands are under the Fermi-level, and four bands are above the Fermi-level. While, $G1^{+1}$ includes three bands, of which, one band is above the Fermi-level, and the others are under the Fermi-level. So the intergroup couplings between $G1^{+1}$ bands and $G2^{+1}$ bands make VB bend upward. Similarly, the intergroup couplings between $G1^{-1}$ bands and $G2^{-1}$ bands make CB bend downward. Then CB and VB intersect, and the DC can be formed by further couplings.

When N is odd, for example, N is three, correspondingly, the intragroup couplings of segment 2 (or segment 1) produce three new bands, of which one band is under the Fermi-level, one band is above the Fermi-level, and one band is near the Fermi-level. The couplings between the new bands from segment 1 and the band from the pair atoms produce four new bands, of which, two bands are under the Fermi-level, two bands are above the Fermi-level. At last, $G2^{+1}$ includes 7 bands shown in Fig. S8 (c, i) with green lines, of which, three bands are under the Fermi-level, three bands are above the Fermi-level, and one band is near the Fermi-level. While, $G1^{+1}$ includes three bands, of which, two bands are under the Fermi-level, and one band is above the Fermi-level. Similarly, there is also a band near the Fermi-level in $G2^{-1}$ which is coincident with the band near the Fermi-level in $G2^{+1}$. And the intergroup couplings between $G1^{+1}$ bands and $G2^{+1}$ bands as well as the intergroup couplings between $G1^{-1}$ bands and $G2^{-1}$ bands do not make the two bands near the Fermi-level (VB and CB) intersect with the similar manner as that of 6,6,12-graphyne. Then, Further couplings

do not form DC along the path $k_y = 0$. The formation process of the band structure of ch-3 is shown in Fig. S8.

These predictions are confirmed by the band structures calculated by DFT shown in Fig. S9.

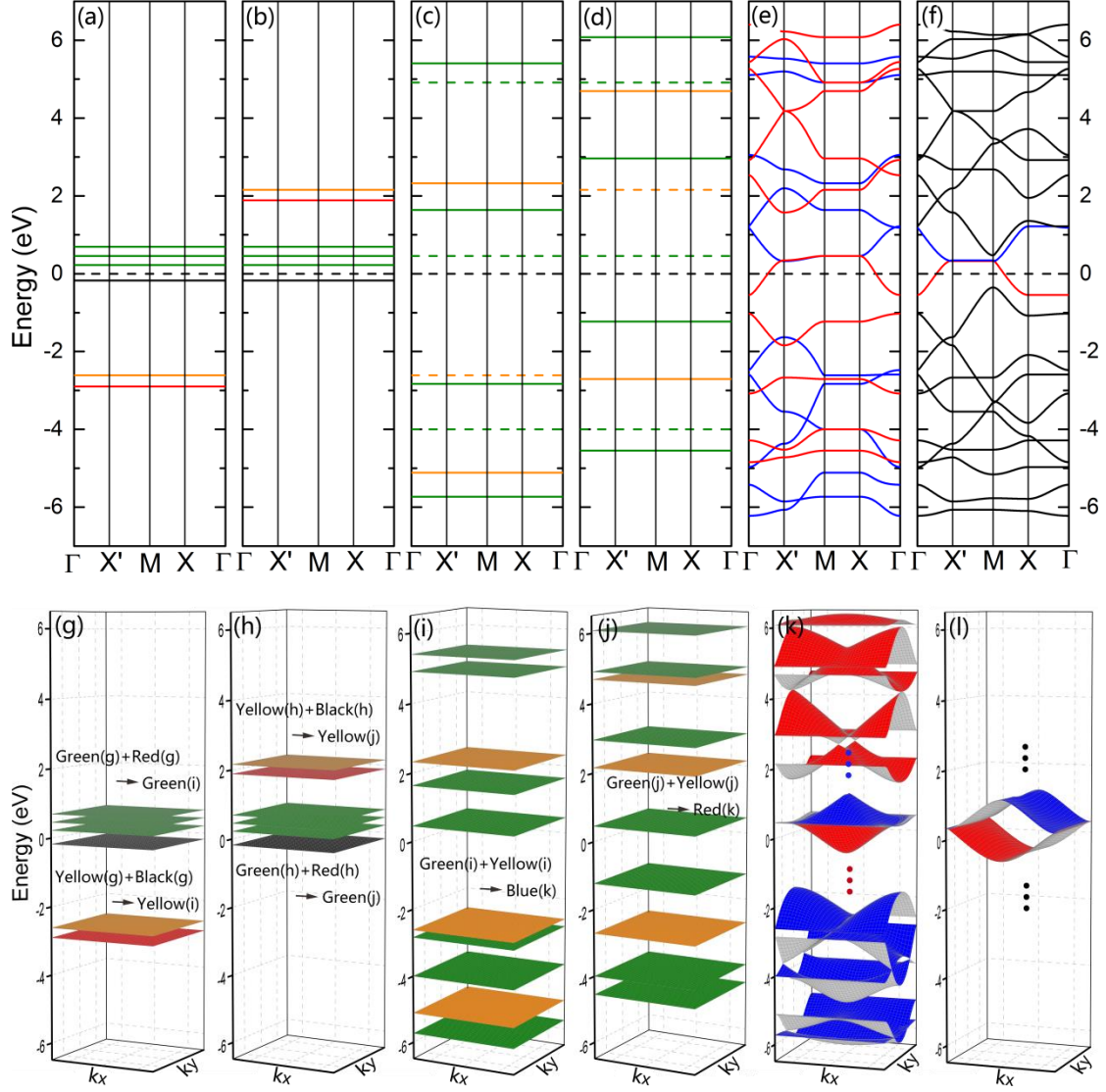


Fig. S8 The formation procession of the band structure of ch-3. (a, g) $G1^+_0$ bands in black, yellow and blue lines and $G2^+_0$ bands in green and red lines. (b, h) $G1^-_0$ bands in black, yellow and blue lines and $G2^-_0$ bands in green and red lines. (c, i) $G1^+_1$ bands in yellow lines and $G2^+_1$ bands in green lines. (d, j) $G1^-_1$ bands in yellow lines and $G2^-_1$ bands in green lines. (e, k) G^+_2 bands in blue lines and G^-_2 bands in red lines. (f, l) The band structure of ch-3 with no DC along the path $\Gamma X'$ is formed with the intergroup couplings between G^+ and G^- considered.

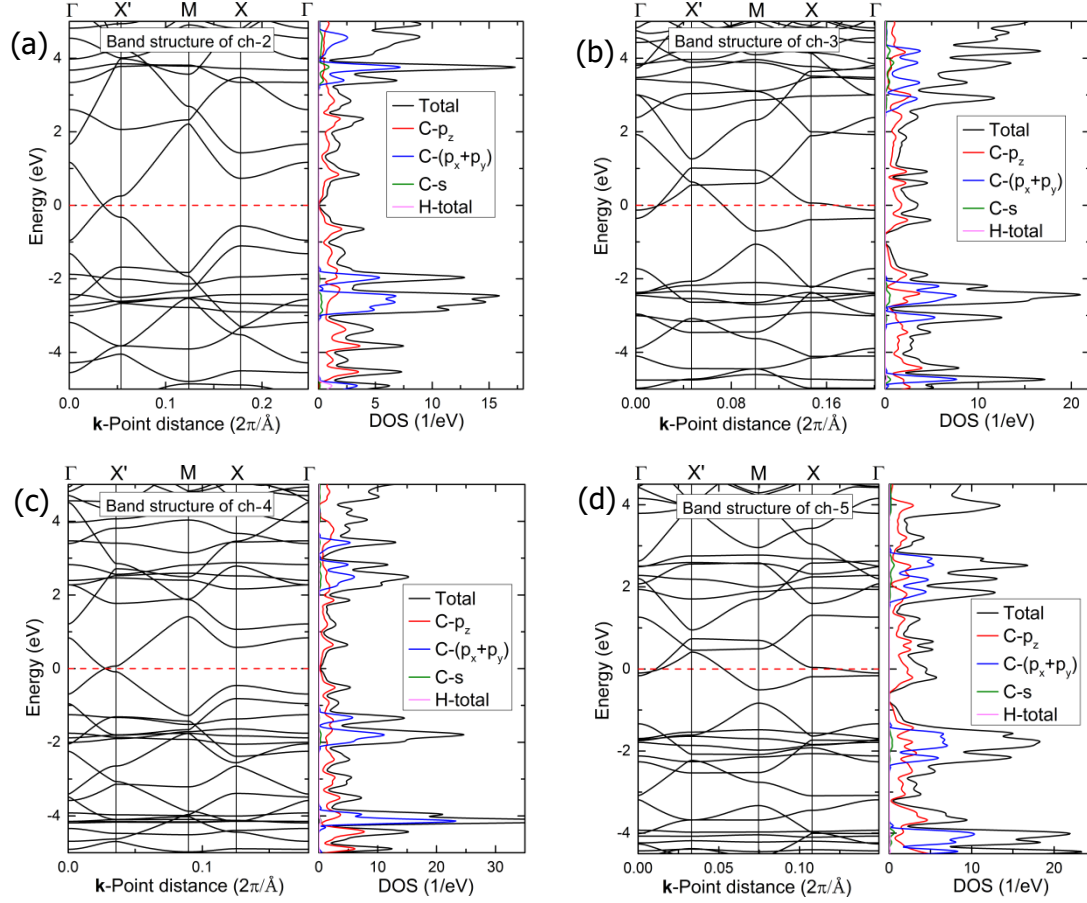


Fig. S9 Band structures of ch-N calculated by DFT.

S3.2 P-N

P-N should possess DC when N is even. When $N=4n$, P-N possesses DC in the path $k_y = \pm\pi/b$, which can be explained as the following. For example $N=4$, $G2^{+0}$ includes six bands, of which, two bands are from “pair” atoms (of which, one band is under the Fermi-level, another band is near the Fermi-level), four bands are from the “chain” atoms and are near the Fermi-level. The four bands from the “chain” atoms can be divided into two segments, segment 1 possesses even parity relative to $x = a/2 + ha$ in each cell, and segment 2 possesses odd parity relative to $x = a/2 + ha$ in each cell. The intragroup couplings of segment 2 (segment 1) produce two new bands shown in Fig. S10 (c) with green dotted lines (green solid lines) and Fig. S10 (i) with green lines, of which, one band is under the Fermi-level, and another band is above the Fermi-level. The intergroup couplings between the new bands from segment 1 and the band from the “pair” atoms which possesses even parity relative to $x = a/2 + ha$ in each cell produce four new bands, of which, two bands are under the Fermi-level, two bands are above the Fermi-level, and the nearest band from the Fermi-level is above the Fermi-level. At last, $G2^{+1}$ includes six bands, of which, three bands are under the Fermi-level, and three bands are above the Fermi-level, and the nearest band from the Fermi-level is above the Fermi-level. While, $G1^{+1}$ includes three bands, of which, two bands are above the Fermi-level, and one band is under the

Fermi-level. So the intergroup couplings between $G1^{+'1}$ bands and $G2^{+'1}$ bands make CB bend downward shown in Fig. S10 (e, k). Similarly, the intergroup couplings between $G1^{-'1}$ bands and $G2^{-'1}$ bands make VB bend upward. Then CB and VB intersect (shown in Fig. S10 (e, k)), and the DC can be formed by further couplings (shown in Fig.S10 (f, l)).

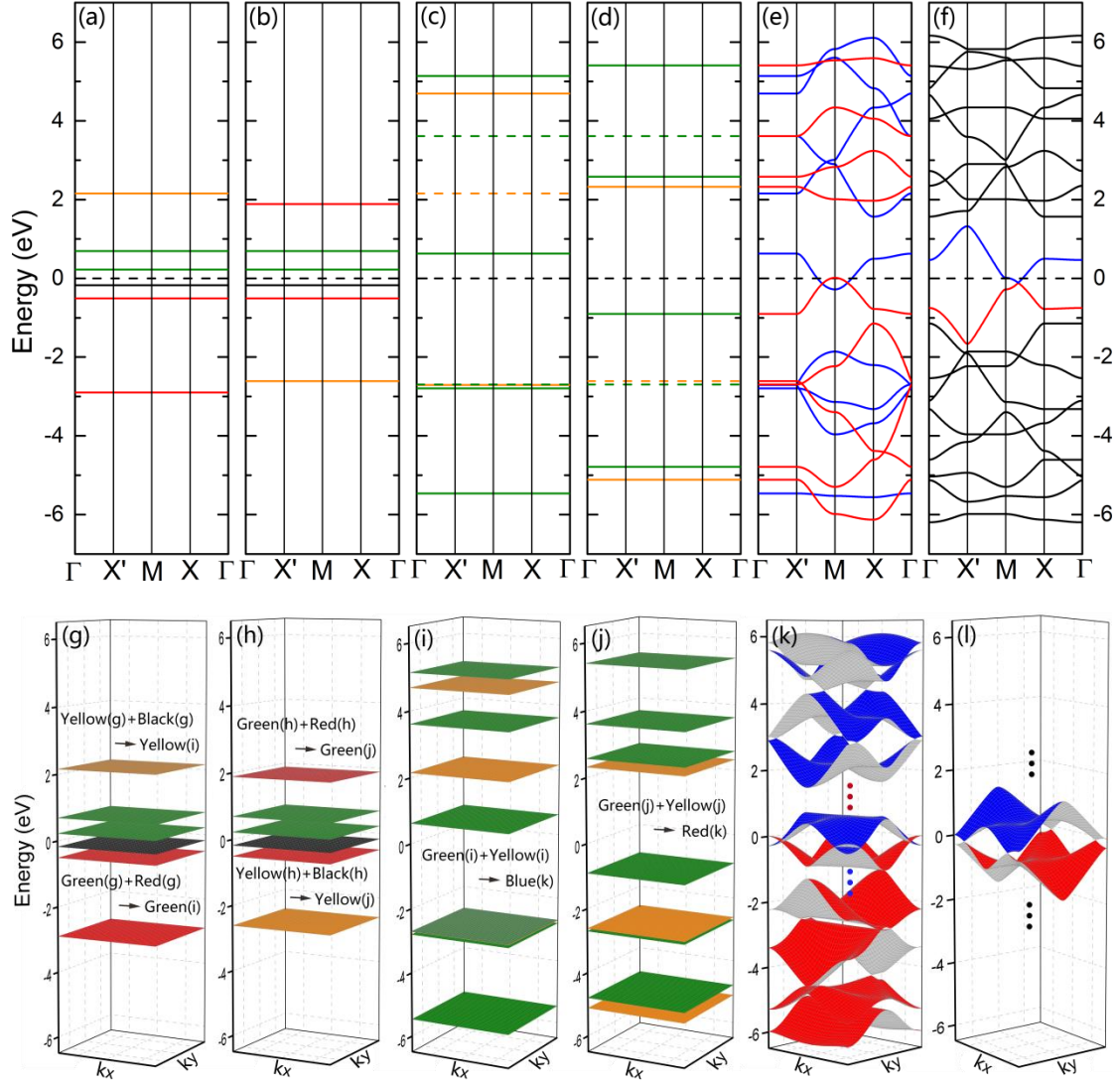


Fig. S10 The schematic formation process of the DC along the path MX of p-4. (a, g) $G1^{+'0}$ bands in black, yellow and blue lines and $G2^{+'0}$ bands in green and red lines. (b, h) $G1^{-'0}$ band in black, yellow and blue lines and $G2^{-'0}$ bands in green and red lines. (c, i) $G1^{+'1}$ bands in yellow lines and $G2^{+'1}$ bands in green lines. (d, j) $G1^{-'1}$ in yellow lines and $G2^{-'1}$ bands in green lines. (e, k) $G^{+'2}$ bands in blue lines and $G^{-'2}$ bands in red lines. (f, l) The band structure of p-4 with DC along the path MX is formed with the intergroup couplings between $G^{+'}$ and $G^{-'}$ considered.

When $N=4n+2$, p-N possesses DC in the path $k_y = 0$. The reason can be explained as the following. In this situation, $G2^{+0}$ (or $G2^{-0}$) include $2n+5$ bands, of which, $2n+1$ bands are from “pair” atoms (of which, one band is under the Fermi-

level, $2n$ bands are near the Fermi-level), four bands are from “chain” atoms and are near the Fermi-level. The four bands from the “chain” atoms can be divided into two segments, segment 1 possesses even parity relative to $x = a/2 + ha$ in each cell, and segment 2 possesses odd parity relative to $x = a/2 + ha$ in each cell. The intragroup couplings of segment 2 (or segment 1) produce two new bands, of which, one band is under the Fermi-level, and another band is above the Fermi-level. The intergroup couplings between the new bands from segment 1 and the band from the “pair” atoms that possess even parity relative to $x = a/2 + ha$ in each cell produce $2n+3$ new bands, of which, $n+2$ bands are under the Fermi-level, $n+1$ bands are above the Fermi-level. At last, $G2^+_1$ includes $2n+5$ bands, of which, $n+3$ bands are under the Fermi-level, and $n+2$ bands are above the Fermi-level, and the nearest band from the Fermi-level is under the Fermi-level. So the original Bloch state vectors should be divided into two groups as eq. (4-7) in the manuscript, which can result that, in $G1^+_1$ bands, two bands are under the Fermi-level, one band is above the Fermi-level. Then the intergroup couplings between $G1^+_1$ bands and $G2^+_1$ bands make VB bend upward. Similarly, the intergroup couplings between $G1^-_1$ bands and $G2^-_1$ bands make CB bend downward, and the DC can be eventually formed along the path $k_y = 0$.

p-N should not possess DC when N is odd with the reason similar to α -N graphyne studied in our previous work². There are odd carbon atoms between the “pair atoms” when N is odd. For each atom between the “pair atoms”, there still is one π (p_\perp) orbital except for the p_z orbitals. The couplings of these p_\perp will form $N-2$ bands, and the middle band is localized near the Fermi-level. The appearance of non- p_z orbital band at Fermi-level leads to the absence of DC at Fermi level.

These predictions are confirmed by the band structures calculated by DFT shown in Fig. S11 and Fig. S9 (a) (ch-2 and p-2 refer to the same structure).

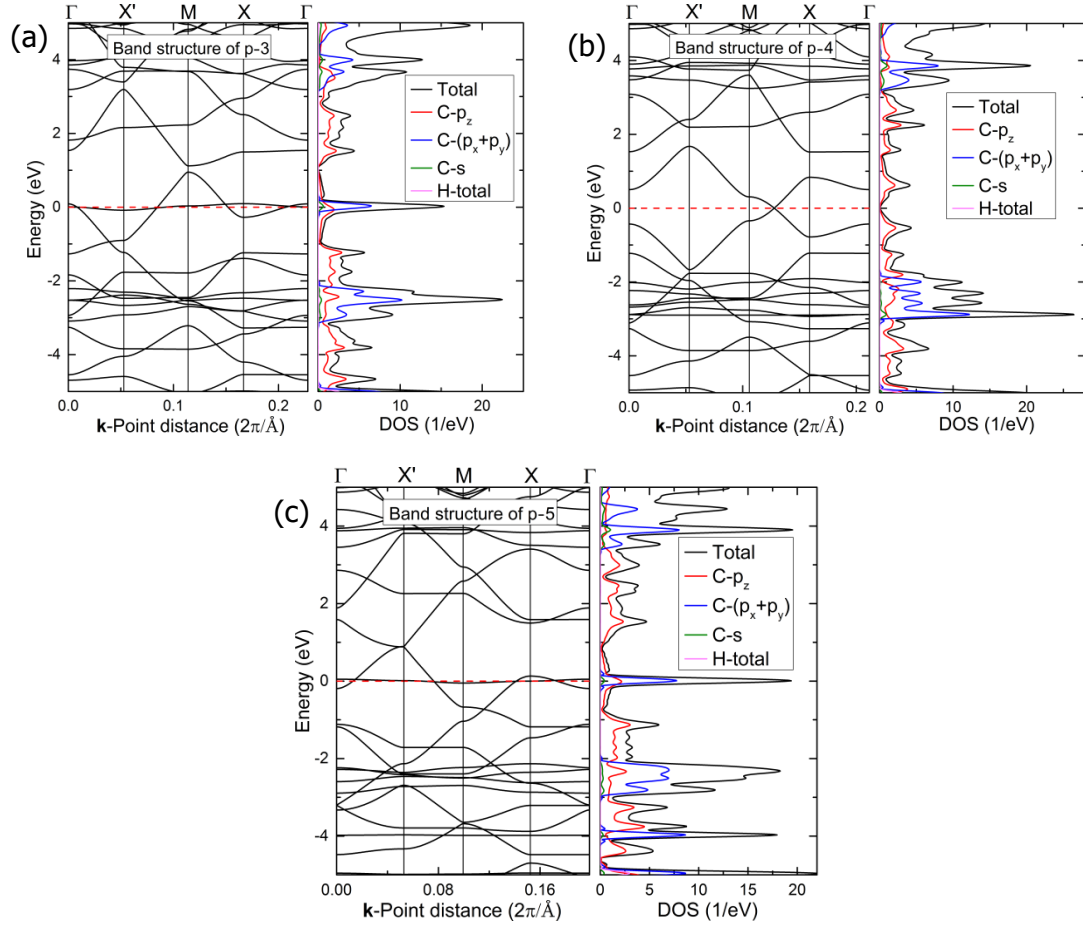


Fig. S11 Band structures of p-N calculated by DFT.

S3.3 sch-N and sp-N

Similar to ch-N and p-N, it can be predicted that sch-N and p-N whether possessing DC or not: sch-N possesses DC in the path $k_y = 0$ when N is even, and do not possesses DC when N is odd; sp-N possesses DC in the path $k_y = 0$ when $N=4n+2$, possesses DC in the path $k_y = \pm\pi/b$ when $N=4n+2$, and do not possesses DC when N is odd. These predictions are confirmed by the band structures calculated by DFT shown in Fig. S12 (sch-2 and sp-2 refer to the same structure).

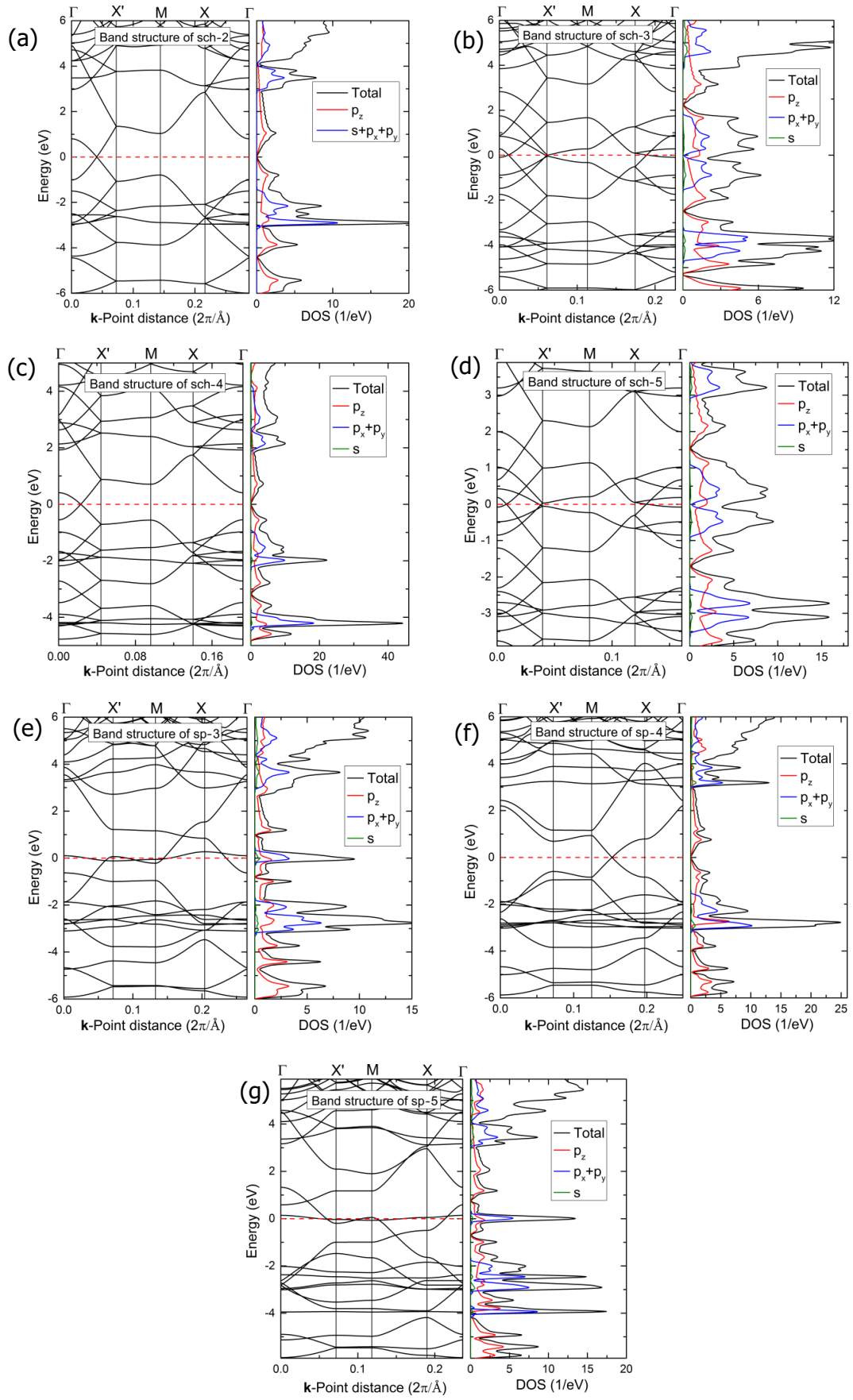


Fig. S12 Band structures of sch-N and sp-N calculated by DFT.

S4 Opening the band gap along the path $k_y = 0$ of 6, 6, 12-graphyne by breaking the mirror symmetry

In order to verify the viewpoint in the manuscript that the breaking of mirror symmetry relative to the x-axis of 6, 6, 12-graphyne would open a gap at the DC point along the path $k_y = 0$, we adjusted the TB parameters to break the mirror symmetry relative to the x-axis of 6, 6, 12-graphyne. **Fig. S13** shows the band structures (along the path $k_y = 0$ and near the DC) by TB of 6, 6, 12-graphyne with various adjusted TB parameters, indicating that the band gap are indeed found after the symmetry is broken.

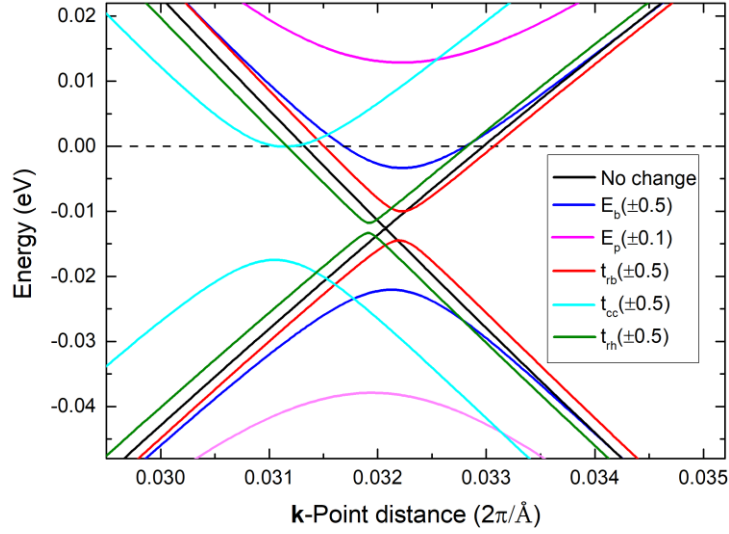


Fig. S13 band structures (along the path $k_y = 0$ and near the DC) by TB of 6, 6, 12-graphyne with various adjusted TB parameters. The legend “ $t_{cc}(\pm 0.5)$ ” indicates that some of t_{cc} parameters are adjusted into $t_{cc}+0.5$ and the rests into $t_{cc}-0.5$. Meanwhile, it should be ensured that the mirror symmetry of the system relative to the x-axis is broken, while the mirror symmetry relative to the y-axis is not broken. The other legends have similar meanings.

References

- (1) D. Malko, C. Neiss and A. Görling, *Phys. Rev. B*, 2012, 86, 045443.
- (2) X. Qin, Y. Liu, B. Chi, X. Zhao and X. Li, *Nanoscale*, 2016, 8, 15223-15232.